

Supporting information for “Temperature-independent rescaling of the local activation barrier drives free surface nanoconfinement effects on segmental-scale translational dynamics near T_g ”

Daniel Diaz-Vela^a, Jui-Hsiang Hung^a, David S. Simmons^b

^aThe University of Akron, 250 South Forge St. Akron OH 44325

^bThe University of South Florida, 4202 E. Fowler Ave., ENB 118, Tampa, FL 33620

Simulation methodology

Simulations employ the short-FENE polymer model¹ that is modified from the standard Kremer-Grest model² to exhibit enhanced crystallization resistance via the shortening of backbone bonds. Prior work has shown that the glass formation behavior of this polymer is similar to that of the standard Kremer-Grest model, including under nanoconfinement^{3,4}. Each chain is comprised of 20 beads, with a total of 10,000, 128,000, and 1,024,000 beads yielding films of thickness 15σ , 47σ , and 97σ respectively. For each size, both a thin film and bulk system are simulated.

Molecular dynamics simulations are performed using LAMMPS (Large-scale Atomic/Molecular Massively Parallel Simulator)⁵. Temperature control is performed via the Nose-Hoover thermostat, as implemented in LAMMPS, with a damping parameter of 2.0. Bulk simulations are performed in the NPT ensemble at zero pressure, employing a Nose-Hoover barostat with damping parameter 2.0 for pressure control. Free-standing film simulations are nominally performed in the NVT ensemble, but the presence of free surfaces yields an effective NPT ensemble for the film. Simulations employ an integration time step size of $0.005\tau_{LJ}$, where τ_{LJ} is the Lennard Jones unit of time. Periodic boundary conditions were applied in all cases except where otherwise noted.

Film simulations were initiated from a random configuration generated in Packmol⁶. This initial configuration was subject to an isothermal equilibration at an initial high temperature ($T = 1.3$, $T = 1.5$, and $T = 1.3$ for the films of thickness 15σ , 47σ , and 97σ , respectively) for a duration of $5000\tau_{LJ}$. During this initial equilibration, boundaries in the box dimension normal to the film surface employed a reflective rather than periodic boundary condition. Film formation was encouraged by employing an anisotropic box with the z dimension considerably larger than the x and y directions, and with a total box volume considerably greater than that required to fit the chosen number of chains at their liquid-state density. In all cases at least 4σ of empty space was maintained above and below the films after film formation, with the box dimension in the direction normal to the interface slightly adjusted with cooling to maintain this amount of space. This adjustment was necessary because of intermittent simulation crashes observed in LAMMPS in the presence of larger void spaces. Bulk systems were generated with an equivalent protocol, but employing a constant pressure boundary condition.

After this initial high temperature equilibration, each system was subject to a thermal quench at a rate of $10^{-4} T/\tau_{LJ}$. Temperatures selected to provide an approximately even spacing in relaxation time are saved during this quench, with each configuration subject to a post-quench equilibration of at least 10 times the segmental relaxation time determined at that temperature. The quench and anneal strategy is a standard approach to achieving equilibrium configurations over a broad range of temperature in recent simulation work studying the glass transition.^{3,4,7-16} Data is then collected over a period of approximately ten times the segmental relaxation time at each temperature to allow accumulation of sufficient statistics.

Simulation analysis

Segmental relaxation time was characterized via the self-part of intermediate scattering function:

$$F_{self}(\mathbf{q}, t) = \frac{1}{N} \sum_j^N \left\langle \exp \left[-i\mathbf{q}(\mathbf{r}_j(t) - \mathbf{r}_j(0)) \right] \right\rangle \quad S1$$

where \mathbf{q} is the wavevector, t is time, N is the number of particles in the system, and $\mathbf{r}_j(t)$ is the position of particle j at time t . This relaxation function was computed at a wavenumber of 7.07, comparable to the first peak in the structure factor, by averaging over many randomly chosen wave vectors comparable to this wavenumber. For interpolation purposes, the results were fitted to the Kohlrausch-Williams-Watts (KWW) stretched exponential functional form^{17,18}. The relaxation time was then defined by convention as the time at which this relaxation function decays to a value of 0.2, consistent with a large body of recent simulation work^{10,19-21}.

In order to determine the positions of the film’s surfaces, each simulation box was divided into 500 bins in z direction and density was computed in each of them. Then, the location of the interface was determined as the location at which the density is equal to half of the bulk density at the same temperature. Finally, the film is divided in layers of 0.875σ measured from each of the interface for analysis of dynamical properties at a local level.

Impact of choice of fitting parameters

The main text presents results of fits of data in Figure 2a to equation 7 employing fixed values of $\varepsilon_h = 0$ and $w = 2$. As shown in Figure S 1, results of a free fit to all parameters support these constraints for $z < 7$. Similarly, the values of the other three parameters are not substantially altered in this range by imposition of this constraint, albeit with a reduction in scatter due to the

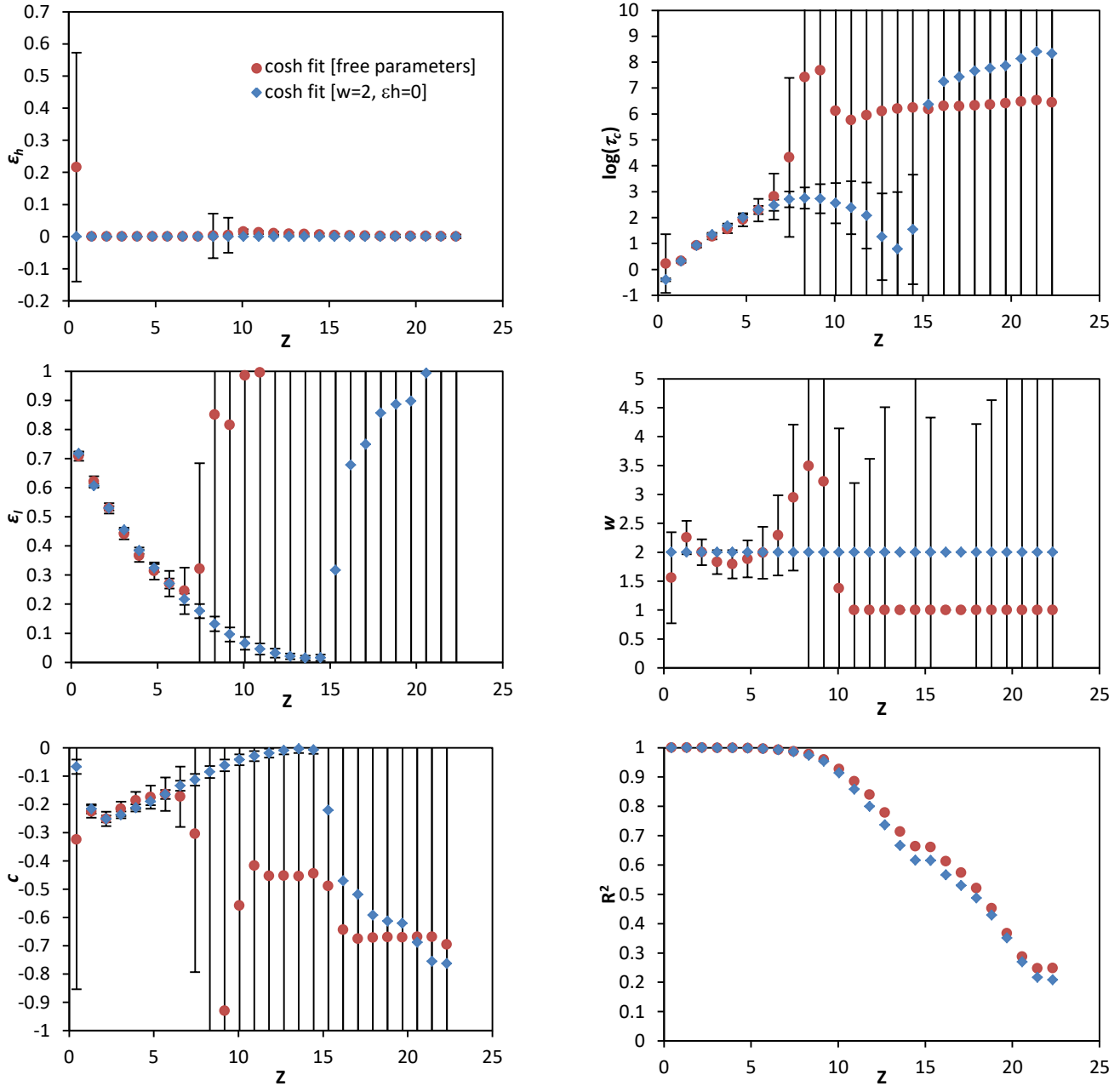


Figure S 1 Fitting parameters for fits of data shown in figure 3 in the main text to equation 7 in the main text, plotted vs the distance z from the interface. Red circles are the parameters of a fit with all parameters in equation 7 treated as adjustable; blue diamonds are parameters for fits constrained to $w = 2$ and $\varepsilon_h = 0$. The latter fit is the one employed in the main text. Error bars are 95% confidence intervals.

reduction in free fit parameters. Beyond $z = 7$, parameter uncertainties become excessively large due to the very weak extent of decoupling observed at these high z .

Robustness of results to choice of functional form

In order to confirm that the finding of a low-temperature plateau is not sensitive to the choice of functional form, we additionally fit the data in Figure 2a of the main paper to several spline forms. We specifically employ several smoothing splines, as implemented in Matlab. Within this implementation, the choice of a smoothing parameter p interpolates between a straight line fit at $p = 0$ and a cubic spline at $p = 1$. We perform fits with

smoothing parameters of $p = 0.4, 0.6,$ and 0.8 . All of these splines yield fits with high R^2 . As in the main paper, we then differentiate these fits to yield a determination of ε as a function of bulk relaxation time. As shown in Figure S 2, all of these splines are in general agreement with the results of the cosh form, with some modest deviations at the shortest relaxation times. All agree qualitatively on the emergence of a plateau in ε at low temperature, corresponding to a low-temperature fractional power law relation between local film dynamics and bulk dynamics.

We additionally seek to ensure that this plateau is not the result of an edge artifact in the fitting process. To do so, we truncate the data in figure 2a in the main manuscript at shorter timescales

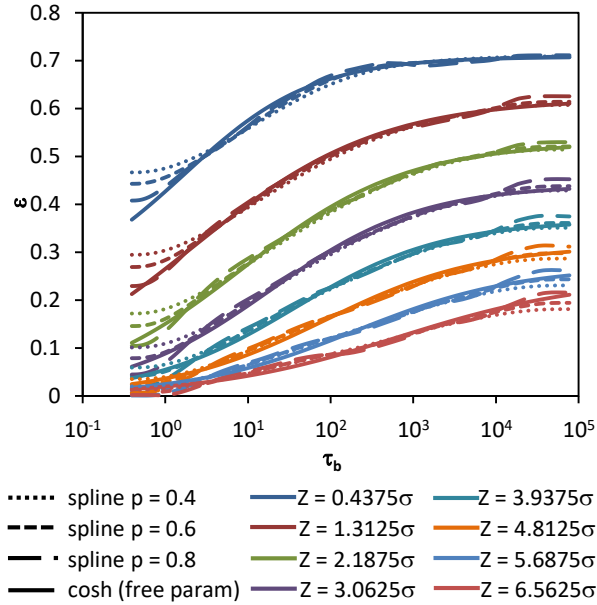


Figure S 2. Comparison of ϵ vs τ_b data as determined via fits to equation 7 in the main text and to several smoothed splines with smoothing parameters indicated in the legend. Distinct line colors represent different distances from the surface, as indicated in the legend.

than the longest available and refit the data to determine whether this leads to an appreciable alteration in the fit to long-time data. As shown in Figure S 3, the results of this truncation process indicate that edge effects are possible within at most the last decade of data included in the fit and are in most cases small in magnitude. This weak magnitude is particularly the case near the surface of the film where the plateau is most well developed within the accessible time range. Since turnover to a long-time plateau is reflected well before the last decade of data included in the fit, fitting edge effects are not a plausible origin of this observation; it is evidently a genuine feature of the data.

Relaxation behavior at long range

Figure 2 in the main text truncates relaxation time data at $z < 7$ to focus on the regime for which deviations from bulk are sufficient to allow analysis with good statistics. To illustrate that dynamics at long range indeed recover their bulk like behavior, in Figure S 4, we extend figure 2 in the main text to include layers deep into the film.

Comparison to temperature shift approaches

As noted in the main text, multiple prior efforts have attempted to describe interface effects on dynamics via various types of temperature shift methods. For example, Napolitano et al employed a position-dependent Vogel temperature²², within an empirical Vogel-Fulcher-Tammann rate law^{23,24}, to describe relaxation data in thin films. Alternately, Forrest and Dalnoki-Veress employed a ‘rheological temperature’ approach wherein the local dynamics within the film at a temperature T are taken to instead be characteristic of bulk dynamics at some other temperature T_r .²⁵

Any means of quantifying shifts in dynamics can formally be recast in terms of a temperature-dependent and thickness-de-

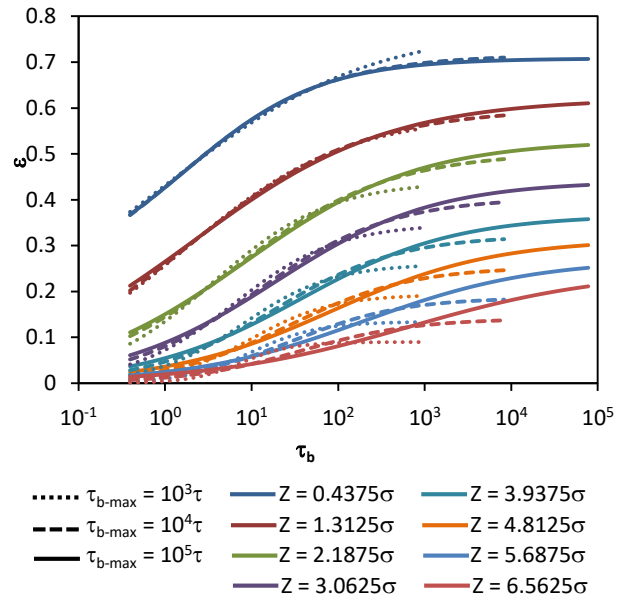


Figure S 3. Comparison of ϵ vs τ_b data as determined via fits to equation 7 in the main text employing data truncated at a maximum bulk timescale of $10^5 \tau_{LJ}$ (the full data set), $10^4 \tau_{LJ}$, or $10^3 \tau_{LJ}$, as indicated in the legend. Distinct line colors represent different distances from the surface, as indicated in the legend.

pendent or position-dependent rescaling of the activation bar-

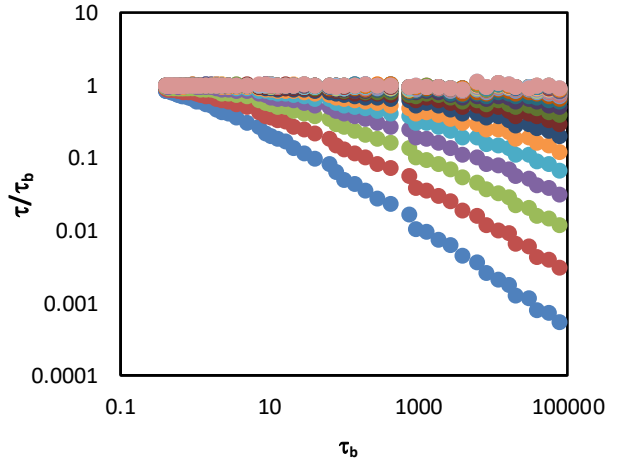


Figure S 4. As in figure 2 of the main text, local film relaxation times normalized by bulk relaxation times at the same temperature, plotted vs bulk relaxation times. The bottom layer is at distance 0.4375σ from the interface, with layer distances progressively increasing in 0.875σ increments upward along the figure.

rier. The key finding in the main manuscript is that this rescaling factor saturates to a constant value below some onset temperature for any given location in the film, such that the barrier in a thin film can be factored into one bulk-like factor that is temperature-dependent only and one surface-sensitive factor that is position-dependent only. Here we show that this finding is unique to the present approach and that previously established temperature-rescaling strategies lead to a barrier rescaling that is both temperature and position dependent.

We begin, consistent with Napolitano et al²² and others^{26,27}, by employing an empirical VFT form with a thickness dependent Vogel temperature to describe thin film dynamics:

$$\tau(T, h) = \tau_{\infty} \exp\left[\frac{BT_0(h)}{T - T_0(h)}\right], \quad (S2)$$

where the breadth parameter B is taken to be unmodified from its bulk value. We can rewrite this in terms of a standard activation model with a temperature-dependent effective barrier,

$$\tau(T, h) = \tau_{\infty} \exp\left[\frac{\Delta E(T, h)}{kT}\right], \quad (S3)$$

where

$$\Delta E(T, h) = BkT \frac{T_0(h)}{T - T_0(h)}. \quad (S4)$$

In the infinite film thickness limit, this must recover the bulk behavior,

$$\tau_B(T) = \tau_{\infty} \exp\left[\frac{\Delta E_B(T)}{kT}\right], \quad (S5)$$

with

$$\Delta E_B(T) = BkT \frac{T_{0B}}{T - T_{0B}}, \quad (S6)$$

where “ B ” subscripts denote the bulk state.

If we combine equations (S3) and (S5) for the thin film and bulk, we can arrive at an expression for the relaxation time reduction in a film of thickness h at a temperature T :

$$\frac{\tau(T, h)}{\tau_B(T)} \propto \exp\left[\frac{\Delta E_B(T)}{kT} \left(\frac{\Delta E(T, h)}{\Delta E_B(T)} - 1\right)\right]. \quad (S7)$$

We can rewrite this in a form similar to equation 4 in the main manuscript:

$$\frac{\tau}{\tau_B} \propto \exp\left[\frac{\gamma(T, h)\Delta E_B(T)}{kT}\right], \quad (S8)$$

where

$$\gamma(T, h) = \frac{T_0(h)}{T_{0B}} \frac{T - T_{0B}}{T - T_0(h)} - 1. \quad (S9)$$

Comparing with the thin film VFT equation above, we can then write this as

$$\Delta E(T, h) = \gamma(T, h)\Delta E_B(T). \quad (S10)$$

Crucially, in contrast to equation 4 in the main manuscript, which has $\gamma = \gamma(T) \neq \gamma(T, h)$, here the rescaling factor on the free energy depends on both thickness (or position) and temperature, such that the thermal and position dependences of the barrier cannot be factored.

In the related rheological temperature approach, the dynamics of the system at a position z within the film are simply treated as behaving as the bulk system but at a modified temperature T_r denoted the rheological temperature, i.e.

$$\tau_B(T) = \tau_{\infty} \exp\left[\frac{\Delta E_B(T)}{kT}\right], \quad (S11)$$

and

$$\tau(T, z) = \tau_{\infty} \exp\left[\frac{\Delta E_B(T_r(z))}{kT_r(z)}\right], \quad (S12)$$

where we can understand the rheological temperature as reflecting a position-dependent temperature ‘adjustment’ ΔT , $T_r(z) = T - \Delta T(z)$. For convenience of comparison with the former approach we now employ an approximate VFT form for the temperature dependence of the relaxation time, yielding

$$\tau(T, z) = \tau_{\infty} \exp\left[\frac{BT_{0B}}{T - T_{0B} - \Delta T(z)}\right]. \quad (S13)$$

Rearrangement of this equation and comparison with the bulk VFT barrier given by equation (S6)

$$\frac{\tau(T, z)}{\tau_B(T)} \propto \exp\left[\frac{\gamma(T, z)\Delta E_B(T)}{kT}\right], \quad (S14)$$

with

$$\gamma(T, z) = \left(1 - \frac{\Delta T(z)}{T - T_{0B}}\right)^{-1}. \quad (S15)$$

Thus this approach again reduces to a barrier of the form given by equation (S10), albeit with an altered form for γ . Crucially, however, the barrier rescaling is again temperature dependent in contrast to equation 4 in the main manuscript.

AUTHOR INFORMATION

Corresponding Author

* dssimmons@usf.edu

Author Contributions

The manuscript was written through contributions of all authors. All authors have given approval to the final version of the manuscript.

ACKNOWLEDGMENT

This material is based upon work supported by the National Science Foundation under Grant No. CBET1705738. The authors acknowledge the W.M. Keck Foundation for generous support enabling development of simulation methodologies employed in this work. The authors thank K. Schweizer for valuable discussions surrounding the idea of spatial decoupling in thin films.

REFERENCES

- (1) Mackura, M. E.; Simmons, D. S. Enhancing Heterogeneous Crystallization Resistance in a Bead-Spring Polymer Model by Modifying Bond Length. *J. Polym. Sci. Part B Polym. Phys.* **2013**, n/a–n/a.
- (2) Kremer, K.; Grest, G. S. Dynamics of Entangled Linear Polymer Melts: A Molecular-dynamics Simulation. *J. Chem. Phys.* **1990**, 92 (8), 5057–5086.
- (3) Mangalara, J. H.; Marvin, M. D.; Wiener, N. R.; Mackura, M. E.; Simmons, D. S. Does Fragility of Glass Formation Determine the Strength of Tg-Nanoconfinement Effects? *J. Chem. Phys. Under Consideration*.
- (4) Mangalara, J. H.; Mackura, M. E.; Marvin, M. D.; Simmons, D. S. The Relationship between Dynamic and Pseudo-Thermodynamic Measures of the Glass Transition Temperature in Nanostructured Materials. *J. Chem. Phys. In revision*.
- (5) Plimpton, S. J. Fast Parallel Algorithms for Short-Range Molecular Dynamics. *J Comp Phys* **1995**, 117, 1–19.

- (6) Packmol: Packing Optimization for Molecular Dynamics Simulations, [Http://Www.Ime.Unicamp.Br/~martinez/Packmol/](http://Www.Ime.Unicamp.Br/~martinez/Packmol/).
- (7) Lang, R. J.; Merling, W. L.; Simmons, D. S. Combined Dependence of Nanoconfined Tg on Interfacial Energy and Softness of Confinement. *ACS Macro Lett.* **2014**, *3*, 758–762.
- (8) Ruan, D.; Simmons, D. S. Glass Formation near Covalently Grafted Interfaces: Ionomers as a Model Case. *Macromolecules* **2015**, *48* (7), 2313–2323.
- (9) Ruan, D.; Simmons, D. S. Roles of Chain Stiffness and Segmental Rattling in Ionomer Glass Formation. *J. Polym. Sci. Part B Polym. Phys.* **2015**, *53* (20), 1458–1469.
- (10) Lang, R. J.; Simmons, D. S. Interfacial Dynamic Length Scales in the Glass Transition of a Model Freestanding Polymer Film and Their Connection to Cooperative Motion. *Macromolecules* **2013**, *46* (24), 9818–9825.
- (11) Riggleman, R. A.; Yoshimoto, K.; Douglas, J. F.; de Pablo, J. J. Influence of Confinement on the Fragility of Antiplasticized and Pure Polymers. *Phys Rev Lett* **2006**, *97*, 0455021–0455024.
- (12) Merling, W. L.; Mileski, J. B.; Douglas, J. F.; Simmons, D. S. The Glass Transition of a Single Macromolecule. *Macromolecules* **2016**, *49* (19), 7597–7604.
- (13) Mangalara, J. H.; Marvin, M. D.; Simmons, D. S. Three-Layer Model for the Emergence of Ultra-Stable Glasses from the Surfaces of Supercooled Liquids. *J. Phys. Chem. B* **2016**, *120*, 4861–4865.
- (14) Betancourt, B. A. P.; Douglas, J. F.; Starr, F. W. Fragility and Cooperative Motion in a Glass-Forming Polymer–Nanoparticle Composite. *Soft Matter* **2012**, *9* (1), 241–254.
- (15) Zhang, W.; Douglas, J. F.; Starr, F. W. Effects of a “Bound” Substrate Layer on the Dynamics of Supported Polymer Films. *J. Chem. Phys.* **2017**, *147* (4), 044901.
- (16) Hanakata, P. Z.; Douglas, J. F.; Starr, F. W. Interfacial Mobility Scale Determines the Scale of Collective Motion and Relaxation Rate in Polymer Films. *Nat. Commun.* **2014**, *5*, 4163.
- (17) Williams, G.; Watts, D. C. Non-Symmetrical Dielectric Relaxation Behaviour Arising from a Simple Empirical Decay Function. *Trans Faraday Soc* **1970**, *66*, 80–85.
- (18) Kohlrausch, F. Kohlrausch. *Pogg Ann Phys.* **1863**, *119*, 352.
- (19) Paul Z. Hanakata; Jack F. Douglas; Francis W. Starr. Local Variation of Fragility and Glass Transition Temperature of Ultra-Thin Supported Polymer Films. *J. Chem. Phys.* **2012**, *137* (24), 244901.
- (20) Hung, J.-H.; Mangalara, J. H.; Simmons, D. S. Heterogeneous Rouse Model Predicts Polymer Chain Translational Normal Mode Decoupling. *Macromolecules* **2018**, *51* (8), 2887–2898.
- (21) Mangalara, J. H.; Simmons, D. S. Tuning Polymer Glass Formation Behavior and Mechanical Properties with Oligomeric Diluents of Varying Stiffness. *ACS Macro Lett.* **2015**, *4* (10), 1134–1138.
- (22) Napolitano, S.; Lupaşcu, V.; Wübberhorst, M. Temperature Dependence of the Deviations from Bulk Behavior in Ultrathin Polymer Films. *Macromolecules* **2008**, *41* (4), 1061–1063.
- (23) Vogel, H. Das Temperatur-Abhängigkeitsgesetz Der Viskosität von Flüssigkeiten. *Phys Zeit* **1921**, *22*, 645–646.
- (24) Fulcher, G. S. Analysis of Recent Measurements of the Viscosity of Glasses. *J Am Ceram Soc* **1925**, *8*, 339.
- (25) Forrest, J. A.; Dalnoki-Veress, K. When Does a Glass Transition Temperature Not Signify a Glass Transition? *ACS Macro Lett.* **2014**, *3*, 310–314.
- (26) Yang, Z.; Fujii, Y.; Lee, F. K.; Lam, C.-H.; Tsui, O. K. C. Glass Transition Dynamics and Surface Layer Mobility in Unentangled Polystyrene Films. *Science* **2010**, *328* (5986), 1676–1679.
- (27) Chowdhury, M.; Guo, Y.; Wang, Y.; Merling, W. L.; Mangalara, J. H.; Simmons, D. S.; Priestley, R. D. Spatially Distributed Rheological Properties in Confined Polymers by Noncontact Shear. *J. Phys. Chem. Lett.* **2017**, 1229–1234.